Real-time Wave Monitoring on Coastal Areas Using LPWAN-Based Embedded Systems

Matias Carandell[1*]
SARTI Group,
Electronic Engineering Department
Universitat Politècnica de Catalunya
Vilanova i la Geltrú, Spain
matias.carandell@upc.edu

Daniel Mihai Toma[1]
SARTI Group,
Electronic Engineering Department
Universitat Politècnica de Catalunya
Vilanova i la Geltrú, Spain
daniel.mihai.toma@upc.edu

Carola Artero
SARTI Group,
Electronic Engineering Department
Universitat Politècnica de Catalunya
Vilanova i la Geltrú, Spain
carola.artero@upc.edu

Manel Gasulla
e-CAT Group,
Electronic Engineering Department
Universitat Politècnica de Catalunya
Castelldefels, Spain
manel.gasulla@upc.edu

Joaquín del Río
SARTI Group,
Electronic Engineering Department
Universitat Politècnica de Catalunya
Vilanova i la Geltrú, Spain
joaquin.del.rio@upc.edu

Abstract— A new embedded system is presented for real-time wave monitoring on coastal areas using SigFox communication. SigFox is a Low-Power Wide-Area Network technology that has been rarely used in coastal marine monitoring. The system is based on the low-power TD1205P module that includes a microcontroller, an accelerometer, a GNSS receiver and a SigFox transceiver. Each hour, the module estimates the wave's maximum height (H_{max}) and mean period (T_z), determines the GPS position, and wirelessly transmits the data through the SigFox network. The procedure for wave parameter estimation is based on the zero-upcrossing method using the vertical acceleration data. It was experimentally validated by attaching the embedded system to a moored buoy and comparing H_{max} and T_z with that provided by a seafloor acoustic wave and current profiler, used as a reference. Results over a period of two months show a good match for H_{max} but less for T_z, which cross-correlation values at zero lag of about 0.85 and 0.5, respectively. Power tests of the embedded system were also performed resulting in a lifetime estimation of 420 days with a battery pack of 3 Ah.

Keywords— *Marine monitoring, Wave Height, Wave Period, Low-Power Wide-Area Network (LPWAN), SigFox, Offshore data transmission, Acoustic Wave And Current profiler (AWAC)*

I. INTRODUCTION

Oceans are a key indicator of earth's health. Small changes in the seawater can have a strong effect on the weather but also on many species' behavior. Thus, oceanographic monitoring becomes essential in terms of understanding biological and meteorological changes. In addition, in-situ measurements provide valuable data which can also be used, among others, to calibrate satellite ocean observation systems [1] or wave forecast models.

Acoustic Wave And Current profilers (AWAC) are in-situ marine instruments commonly used in shallow waters and placed at the sea bottom to measure waves and sea currents profiles, collecting data from waves such as their height, period and direction. Underwater deployments, though, are usually associated with high-costs. Furthermore, to monitor real-time data from an AWAC, a moored buoy with wireless communication or an underwater link [2] are also required, which further increases the costs. Coastal waves can also be measured with HF radar systems [3]. Nevertheless, this infrastructure also implies high costs and cannot be deployed in all coastal areas.

Small moored and free-drifting buoys equipped with embedded Inertial Measurements Units (IMU) also estimate wave parameters. These small-size solutions require lower energy than previous ones, so they can achieve long term power autonomy with primary batteries or even use solar panels to achieve "perpetual" power. In [4], a surface buoy for wave and current studies was presented, where Iridium satellite communication was used. A similar system was presented in [5], where several small-size buoys powered with PV cells were moored in coastal areas. Even so, in these solutions, the satellite communication module is the most energy consuming part and significantly increases the budget both for the module initial cost and for that related with the data transmission (paid service).

Nowadays, Low-Power Wide Area Networks (LPWAN) are starting to be used in coastal marine monitoring because they provide small data transmission packages with relatively low power and costs. Among them, LoRa and SigFox excel [6]. In [7], LoRa communication was used to transmit temperature and humidity from an Indonesian island and in [8] the authors showed data transmission over the sea at distances up to 28 km by placing expensive antennas between 50 and 100 meters above the sea level. In [9], LoRa was proposed in coastal drifting buoys equipped with an embedded system to acquire the wave parameters. However, this system has not been fully implemented yet. On the other hand, SigFox provides longer communication ranges than LoRa [6], becoming more suitable for marine offshore applications. And although the payload of SigFox messages is smaller than in LoRa, so that just small amounts of data can be transmitted, this is enough for remote marine wave monitoring. But just few works can be found using SigFox, as the one presented in [10], which aimed to track endangered salmons on Sweden river zones.

In this paper, we designed and tested a low-cost and low-power embedded system to estimate in real time some wave

This work was supported by the Spanish Ministry of Economy and Competitiveness and the European Regional Development Fund under project TEC2016-76991-P and by the project MELOA from the European Commission's Horizon 2020 research and Innovation program under Grant Agreement No. 776280. The first author has a grant from the Secretariat of Universities and Research of the Ministry of Business and Knowledge of the Government of Catalonia on the FI program (ref. BDNS 362582).

[1] These authors contributed equally to this work.

* Corresponding author.

parameters at coastal areas using SigFox LPWAN technology. It is a smaller and more compact solution than the ones proposed in [9] and [10] and is less energy consuming than [4] and [5]. The paper is organized as follows. First, the estimation of the selected wave parameters is described in Section II. Section III describes the materials and method used to evaluate the proposed system, and the results are summarized and discussed in section IV. Finally, Section V concludes the work.

II. Estimation of the Wave Parameters

Wave parameters can be estimated by evaluating the time series of the sea surface elevation (D_z) from a single point. The zero-upcrossing technique [11] uses the Still Water Level (SWL) reference from the time series data to obtain the height (H) and period (T) of each wave, as represented in Fig. 1. The SWL is the sea surface level in the absence of wind and waves. Then, multiple common parameters can be obtained such as the significant wave height (H_3), which is the mean height of the third highest waves in the record, and the significant wave period (T_3), which is the corresponding mean period. The maximum wave height (H_{max}) is the largest measured wave in the record and the mean zero-upcrossing wave period (T_z) is obtained by

$$T_z = \frac{T_r}{N_z} \tag{1}$$

where T_r is the time length of the record and N_z is the number of zero-upcrossings in that record, considering the SWL as the zero level ($D_z = 0$).

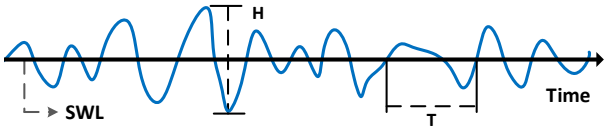

Fig. 1. Time series of the sea surface elevation (Dz), where the Still Water Level (SWL) is used in the zero-upcrossing method to obtain the wave height (H) and period (T).

In [12], we presented a drifting buoy prototype with a measuring system that included an IMU. The buoy was deployed on a Wave-Flume and the IMU raw data was recorded and later processed off-line with a MATLAB algorithm to obtain the wave parameters with the zero-upcrossing technique. There, D_z was obtained from the vertical acceleration (a_z), which is the normal procedure with floating buoys [13]. However, unlike in [12], an IMU is not available in the embedded system used in this paper (to be described in Section III) but just a 3-axis accelerometer, so the gyroscope data cannot be used to correct the potential tilt of a_z. This simplification was also used in [13] and proved to be accurate enough. Furthermore, due to memory and processing constraints, only H_{max} and T_z are provided here. Fig. 2 shows the steps followed to estimate them for each record.

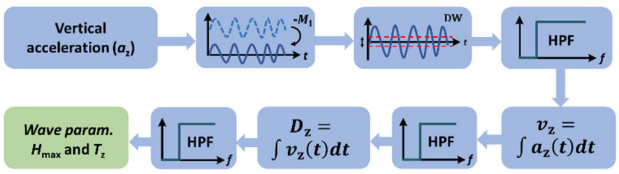

Fig. 2. Steps for the estimation of the wave parameters H_{max} and T_z.

First, the gravity effect is removed from a_z by subtracting its mean value, incrementally calculated as

$$M[i] = \frac{(i-1)M[i-1] + a_z[i]}{i} \tag{2}$$

Second, a discrimination window (DW), consisting on assigning a zero value to values of $a_z \leq 5$mg, smooths out accelerometer's errors due to vibration and mechanical noise during flat sea states. Third, a digital first-order high-pass filter (HPF) removes the slow motion of the infra-gravity waves (e.g. larger than 30 s), resulting in the wave orbital acceleration. The implementation of the HPF in discrete-time is given by

$$y[i] = \alpha \cdot (y[i-1] + x[i] - x[i-1]) \tag{3}$$

where $x[i]$ and $y[i]$ are the data set of samples before and after the HPF, respectively, i is the number of the current sample and α is given by

$$\alpha = \frac{1}{1 + 2\pi f_c T_s} \tag{4}$$

where T_s is the sampling period of the accelerometer data and f_c is the cut-off frequency of the HPF. Fourth, the vertical velocity v_z is obtained performing a numerical time integration given by [14]

$$v_z[i] = v_z[i-1] + \frac{a[i-1] + a[i]}{2} T_s \tag{5}$$

with the first value forced to zero. Again, (3) is used to filter v_z and D_z is obtained by integrating the velocity using

$$D_z[i] = D_z[i-1] + \frac{v_z[i-1] + v_z[i]}{2} T_s \tag{6}$$

with the first value forced to zero. Then, (3) is subsequently applied. Overall, applying three concatenated HPF better removes the slow motion of infra-gravity waves.

Finally, T_z is obtained using (1) and H_{max} is determined from the difference of the maximum and the minimum values of D_z for each time interval T_r.

III. Materials and Method

A TD1205P tracker module (TDnext) was used to obtain H_{max} and T_z and wirelessly transmit the data. It was selected because of its low power consumption and reduced size (30×38×10.5 mm). Fig. 3 shows a block diagram of the module, which includes an EFM32G (32-bit ARM Cortex-M3-based) microcontroller unit (MCU), an ultra-low power 3D Accelerometer, a Hall-Effect sensor (not used here), a GNSS receiver, and a SigFox communication transceiver. A range of ± 8 g for the accelerometer and an output transmission power of +16 dBm for the SigFox transceiver were selected. The SigFox transceiver allows to send up to 140 messages of 12 bytes per day.

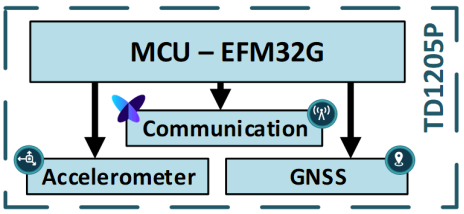

Fig. 3.TD1205P block diagram including the MCU, the accelerometer, and the communication and GNSS modules.

The TD1205P module was programed to wake up every hour. After wake-up, the execution routine is divided in five

stages: 1) acquires 5 min (T_r = 300 s) of a_z at 5 Sa/s (T_s = 200 ms), resulting in 1500 data samples; 2) calculates H_{max} and T_z using the algorithm described in Section II with f_c = 1/15 Hz in order to remove the infra-gravity waves; 3) determines the GPS position with an acquisition time that depends on the current ephemeris and is limited to 60 s to avoid excessive power consumption; 4) sends the data through the SigFox network in a 12 bytes message that includes H_{max}, T_z, an internal temperature, the battery voltage, and the GPS latitude and longitude; and 5) returns to sleep mode. Fig. 4 shows the structure of the hexadecimal coded message. Latitude and Longitude bytes are 0 whenever the GPS position cannot be fixed.

Fig. 4. 12 bytes SigFox message. From left to right, GPS Latitude (4 bytes) and Longitude (4 bytes), battery voltage (1 byte), internal temperature (1 byte), H_{max} (1 byte), and T_z (1 byte).

The TD1205P module was encapsulated within an IP64 case (83×35×57 mm) that also included two 3V batteries (CR123A, GP Batteries) connected in parallel through two Schottky diodes (PMEG1020EA), as shown in Fig. 5. The batteries powered the TD1205P module providing an overall capacity of around 3 Ah at a nominal voltage of 3 V.

Fig. 5. TD1205P module encapsulated with two CR123A 3V batteries within an IP64 case (83×35×57 mm).

A power consumption test that included the five steps following a wake-up was performed to estimate the lifespan of the TD1205P module. The EFM32TG (Energy Micro) Starter Kit was used for this purpose. This kit contains an energy monitoring interface that allows the measurement of current and voltage. Current range is from 0.1 µA to 50 mA with accuracies of 1 µA and 100 µA for values lower and higher than 200 µA, respectively. Resolution in the sub 200 µA range is 100 nA. Results are shown in Section IV.A.

The algorithm for the estimation of the wave parameters was preliminary debugged using the OrcaFlex simulator (Orcina). In [12] we describe how we modeled a drifting buoy and the sea environmental parameters using this tool. Then, the algorithm was validated on a real sea test by comparing the TD1205P results (H_{max} and T_z) with that provided by a seafloor AWAC (1 MHz – Nortek) used as a reference, which presents an accuracy of 1 % on the wave height estimation. To do so, the encapsulated system of Fig. 5 was attached to the upper part of a moored buoy placed at 4 km off the coast of the city of Vilanova i la Geltrú [15]. This buoy is above a 20 meters depth underwater cabled observatory (OBSEA) to which the AWAC is connected. The configuration and work principle of this sensor is described in [2]. Mainly, it acquires 10 minutes of wave data each hour, calculates the wave parameters and transmits the data through the OBSEA network. Both, the encapsulated TD1205P module and the AWAC, were deployed during the summer of 2020. Data H_{max} and T_z were acquired during several weeks between the months of July and October and later compared. Results are shown in Section IV.B.

IV. Experimental Results

A. Power consumption

Fig. 6 shows the supply voltage and current profile of the TD1205P module acquired every 10 ms. Voltage is 3.3 V and a logarithmic scale is used for current to account for the large dynamic range. Stages 1 to 5 occur sequentially, with stage 5 also taking place between stages 2 and 3. TABLE I summarizes the average value of the measured current for each stage as well as the associated time durations and electrical charges. As can be seen, the main two contributors are stages 3 (GPS) and 4 (SigFox data transfer) whereas the charge wasted in the rest of stages is negligible. For stage 3 an average time of 30 s, after several tests in near-real conditions, has been considered. With these conditions, the batteries will last about 420 days, assuming their full capacity of 3 Ah.

A significant battery lifetime increase could be achieved by decreasing the duration of stage 3, e.g. by shifting the estimation of the GPS position from the device to a database. This is a paid service offered by some companies [16] but it cannot be implemented in the SigFox modules of TDnext, such as the TD1205P. Another option would be to save the current ephemeris during the sleep mode. As reported in [17], stage 3 can be reduced down to about 4 seconds at the cost of increasing the current consumption of stage 5 up to 16 µA. However, ephemeris is valid for only 4 hours, hence it must be updated regularly (average time duration of 30 s, TABLE I). Overall, the battery lifetime would be just nearly doubled. Nevertheless, more experimental tests about this issue should be carried out.

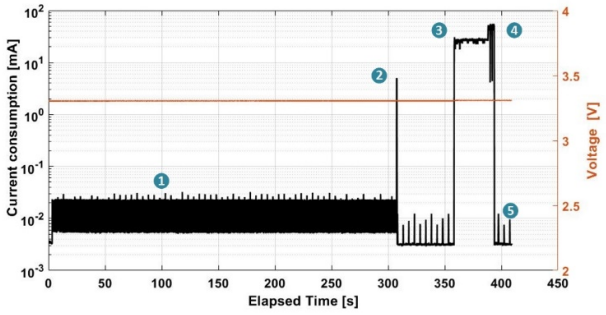

Fig. 6. Supply voltage and current profile of the TD1205P module.

TABLE I. Supply average currents and associated times and charges of the TD1205P module.

Ref	Current (A)	Time (s)	Charge (C)
1	14 u	300	4.2 m
2	3.7 m	0.5	1.85 m
3	26.4 m	30	792 m
4	46.5 m	5.5	256 m
5	3 u	3264	10 m
1-5	0.29 m (average)	3600	1.07

B. *Wave monitoring*

Fig. 7 and Fig. 8 show the time series values of H_{max} and T_z during the sea test. As can be seen, H_{max} and T_z exceed 4 m and 10 s, respectively, in some specific episodes. On the other hand, there are missing data from the AWAC at the beginning of the time series due to a later deployment than the TD1205P module and afterwards (mainly during September) due to communication failures. In the overlapped intervals, the data of both sensors mainly match, in particular that of H_{max}. More quantitatively, the mean of H_{max} and T_z are 0.87 m and 3.34 s, respectively, for the TD1205P, and 0.82 m and 3.20 s for the AWAC, thus showing a good agreement.

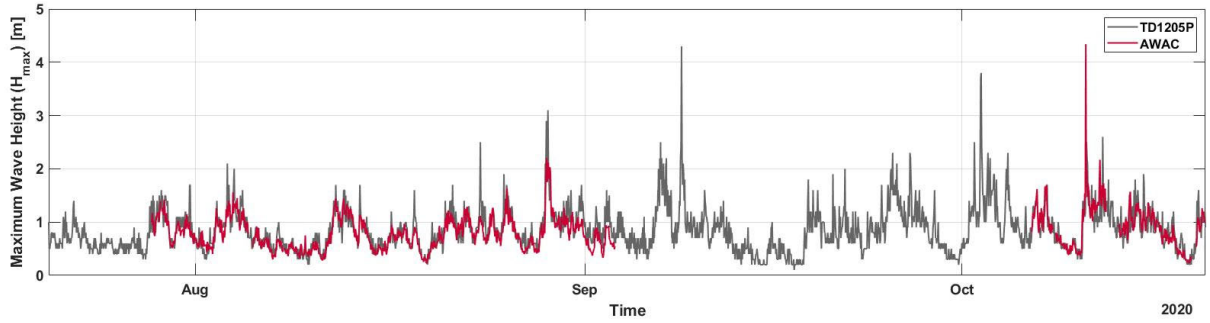

Fig. 7. Experimental values of H_{max} acquired each hour with the TD1205P module (grey) and with the AWAC (red) for 3 months, starting at July 20, 2020. Note some missing data from AWAC measurements due to a communication failure.

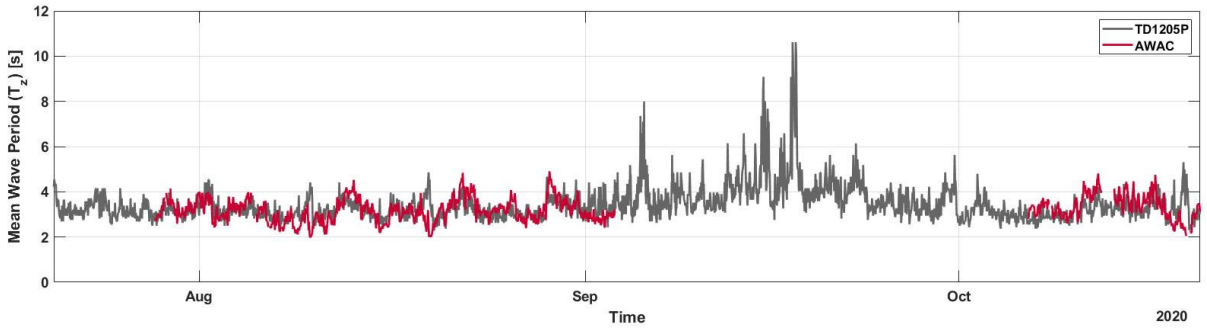

Fig. 8. Experimental values of T_z acquired each hour with the TD1205P module (grey) and with the AWAC (red) for 3 months, starting at July 20, 2020. Note some missing data from AWAC measurements due to communication failures.

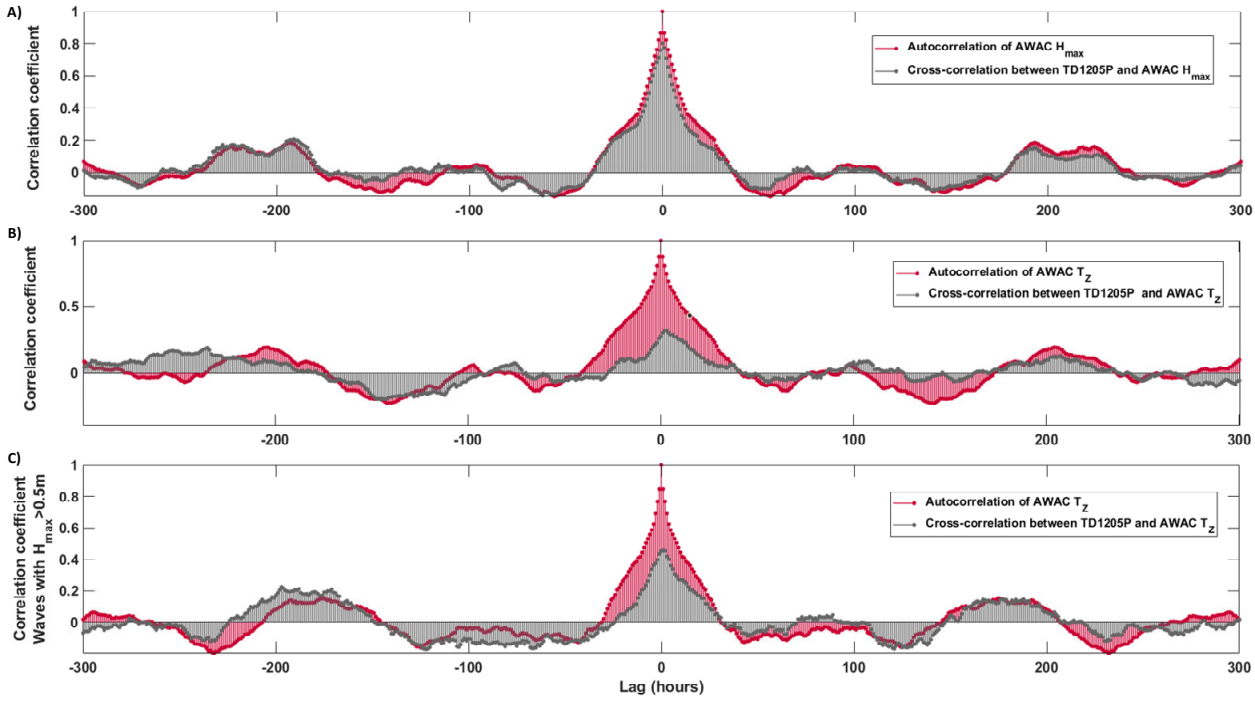

Fig. 9. Correlation analysis for A) H_{max}, B) T_z, and C) T_z when $H_{max} > 0.5$m. In all plots, Auto-correlation is performed using the AWAC temporal series as a reference (in red) and Cross-correlation using the AWAC and TD1205P temporal series (in grey).

Further statistical methods are next presented to better assess the matching between the parameters of the TD1205P and the AWAC. In particular, this analysis was performed using the MATLAB cross-correlation function from the Econometrics Toolbox [18]. Only the data of the overlapped intervals in Fig. 7 and Fig. 8 were used.

Fig. 9-A shows the correlation analysis of H_{max} with lags up to ±300 h, where the sample auto-correlation of the AWAC time series is shown in red and the sample cross-correlation between the AWAC and TD1205P time series in grey. Comparing the auto-correlation of a reference signal (AWAC) with the cross-correlation of this reference with another target signal (TD1205P) for different lags is useful for gaining insight in their similarity and where the best match occurs [19]. As can be seen, both sample correlations present a high overall resemblance, with a maximum cross-correlation value at zero lag (∼0.85), which also indicates the synchronization of both time series [20]. Thus, the estimation procedure of H_{max} with the TD1205P is feasible.

Fig. 9-B shows the correlation analysis of T_z. Similarity between the sample correlations is lower here. Still, both time series are synchronized because the maximum cross-correlation value is at zero lag, though below 0.4. At Fig. 9-C, only T_z values corresponding to $H_{max} > 0.5$ m measured with the AWAC were considered. As can be seen, the cross-correlation value at zero lag increases to ∼0.5, stating that the TD1205P estimates better T_z when sea is rough. Further research is required to state the reason for this behavior.

V. Conclusions

A new embedded system has been designed and tested to estimate the wave's maximum height (H_{max}) and mean period (T_z) and transmit them wirelessly using the LPWAN SigFox network. The system, based on a TD1205P module, obtains the sea surface displacement from the embedded accelerometer and calculates H_{max} and T_z through the zero-upcrossing method.

The wave estimation method has been validated by attaching the embedded system to a moored buoy placed above an acoustic wave and current profiler, used as a reference. Both systems have provided H_{max} and T_z each hour during a period of three months. The mean values of H_{max} and T_z have been 0.87 m and 3.34 s, respectively, for the TD1205P, and 0.82 m and 3.20 s for the AWAC, thus showing a good agreement. A cross-correlation analysis has also been performed, resulting in a high cross-correlation value at zero lag of 0.85 for H_{max}. However, a lower value (< 0.4) is obtained for T_z. Considering only T_z values corresponding to $H_{max} > 0.5$ m, the cross-correlation value has increased to ∼0.5. Further research is required on this issue.

The power consumption of the TD1205P has also been measured, being the GPS location stage the most energy demanding. Using a 3 Ah battery, a lifetime autonomy of 420 days is predicted. A couple of techniques to reduce the consumption of the GPS location stage have been presented to be further explored.

Acknowledgment

The authors extend their thanks to Orcina for their kind support and offer of the academic license OrcaFlex N2703 (2021) to Universitat Politècnica de Catalunya.

References

[1] R. Scharroo *et al.*, "Jason continuity of services: continuing the Jason altimeter data records as Copernicus Sentinel-6," *Ocean Sci.*, vol. 12, no. 2, pp. 471–479, 2016.

[2] M. Carandell and M. Nogueras, "Data comparison between three acoustic doppler current profilers deployed in OBSEA platform in north-western Mediterranean," *Instrum. Viewp.*, no. 19, pp. 87–89, 2016.

[3] J. B. D. Jaffrés and M. L. Heron, "Wave climate in the Southern Great Barrier Reef, Australia - Evaluation of an ocean HF radar system and WaveWatch3," in *OCEANS - Kona Hawaii*, 2011, pp. 144–149.

[4] P. V. Guimarães *et al.*, "A surface kinematics buoy (SKIB) for wave-current interaction studies," *Ocean Sci.*, vol. 14, no. 6, pp. 1449–1460, 2018.

[5] K. Raghukumar, G. Chang, F. Spada, C. Jones, T. Janssen, and A. Gans, "Performance Characteristics of 'Spotter', a Newly Developed Real-Time Wave Measurement Buoy," *J. Atmos. Ocean. Technol.*, vol. 36, no. 6, pp. 1127–1141, 2019.

[6] K. Mekki, E. Bajic, F. Chaxel, and F. Meyer, "Overview of Cellular LPWAN Technologies for IoT Deployment: Sigfox, LoRaWAN, and NB-IoT," *PerIoT'18 - Second IEEE Int. Work. Mob. Pervasive Internet Things*, pp. 413–418, 2018.

[7] N. A. Azmi Ali and N. A. Abdul Latiff, "Environmental Monitoring System Based on LoRa Technology in Island," in *IEEE International Conference on Signals and Systems - Bandung*, 2019, pp. 160–166.

[8] N. Jovalekic, V. Drndarevic, E. Pietrosemoli, I. Darby, and M. Zennaro, "Experimental study of LoRa transmission over seawater," *Sensors*, vol. 18, no. 9, 2018.

[9] I. B. Shirokov, A. S. Mironov, and A. N. Grekov, "Ocean Surface State Monitoring with Drifters Array," in *Zooming Innovation in Consumer Technologies Conference - Novi Sad*, 2020, pp. 113–117.

[10] M. Blinge, "Construction of an IoT-device transmitting data of the endan- gered Atlantic salmon via Sigfox-LPWAN," *Master's Thesis. Chalmers University of Technology*. 2019.

[11] Z. Demerbilek, "Water Wave Mechanics," in *Coastal Engineering Manual*, vol. Part II, 2008.

[12] M. Carandell, D. M. Toma, J. P. Pinto, M. Gasulla, and J. del Río, "Impact on the Wave Parameters Estimation of a Kinetic Energy Harvester Embedded into a Drifter," in *OCEANS - Singapur and U.S. Gulf Coast*, 2020.

[13] E. D. Skinner, M. M. Rooney, and M. K. Hinders, "Low-cost wave characterization modules for oil spill response," *J. Ocean Eng. Sci.*, vol. 3, pp. 96–108, 2018.

[14] K. Seifert and O. Camacho, "Implementing positioning algorithms using accelerometers," *App. Note, Free. Semicond. -NXP*, pp. 1–13, 2007.

[15] E. Molino *et al.*, "Oceanographic Buoy Expands OBSEA Capabilities," *Instrum. Viewp.* -, vol. 11, pp. 14–15, 2011.

[16] Ubiscale, "UbiGNSS: low-power geolocation." [Online]. Available: https://ubiscale.com/.

[17] M. Carandell, D. Mihai, J. del Río, K. Ganchev, and J. Peudennier, "Evaluation of Sigfox LPWAN technology for autonomous sensors in coastal applications," *Instrum. Viewp.*, vol. 20, pp. 36–37, 2018.

[18] MATLAB, "Cross-correlation function." [Online]. Available: https://es.mathworks.com/help/econ/crosscorr.html.

[19] B. Croke, P. Cornish, and A. Islam, "Modeling the Impact of Watershed Development on Water Resources in India," in *Integrated Assessment of Scale Impacts of Watershed Intervention: Assessing Hydrogeological and Bio-Physical Influences on Livelihoods*, Elsevier Inc., 2015, pp. 99–148.

[20] J. Cryer and K. Chan, *Time series analysis: with applications in R*, vol. 2. 2008.